

# Chapter 9

## Removal of Arsenic from Water Using Graphene Oxide Nano-hybrids



Sharf Ilahi Siddiqui, Rangnath Ravi and Saif Ali Chaudhry

**Abstract** In 21st century, providing the fresh and affordable water through protects and purifying the water source from pollutants is biggest and most concern environmental challenges. Toxic element particularly arsenic in water is serious matter of threat for human from many developing countries, and long exposure of arsenic is generally associated with skin lesions and hyperkeratosis like adverse effects. Graphene oxide (GO) and its composites have attracted widespread attentions as novel adsorbents for the adsorption of various water pollutants due to their unique physicochemical characteristics. This chapter presents advances made in the synthesis of graphene oxides and their composites, and summarizes the application of these materials as a superior adsorbent for the removal of arsenic from water. The adsorption affinity in terms of contact time, pH, and temperature has been discussed. Competitive ion effect and regeneration are included within the text. Moreover, the challenges for the commercial uses are discussed.

**Keywords** Heavy metal · Arsenic · Adsorption · Graphene oxide  
Magnetic graphene oxide · Remediation of arsenic

### 1 Introduction

Human life and lives of other animals depend on water; therefore, it is a vital concern for mankind. 71% of the earth's surface is covered up with water but only 2.5% water is fresh. Fresh water in the form of glacial is unusable, thus only ground

---

S. I. Siddiqui · R. Ravi · S. A. Chaudhry (✉)  
Department of Chemistry, Jamia Millia Islamia University,  
New Delhi 110025, India  
e-mail: saifchaudhry09@gmail.com

S. I. Siddiqui  
e-mail: sharf\_9793@rediff.com

R. Ravi  
e-mail: rangnathravi@gmail.com

**Table 1** Some heavy metals and their toxic effect

Heavy metal	Major activities	Effect	References
Lead	Auto mobile, coal burning, smoking, paint and pesticides	Mental retardation in children, liver and kidney failure and cancer	Kumar et al. (2014), Dikilitas et al. (2016)
Mercury	Pesticides, batteries, paper industries	Neurological effect	Ha et al. (2017), Li et al. (2015)
Cadmium	Welding, pesticides, nuclear fusion plant, electroplating	Cancer, kidney damages and gastrointestinal disorder	Fristachi and Chaudhry (2017), Rodríguez and Mandalunis (2016)
Arsenic	Mining, smelting and fertilizers	Renal, dermal, mutagenic, carcinogenic, cardiovascular, and neurological effect	Siddiqui and Chaudhry (2017a, b, c), Rasheed et al. (2017)

and surface water is available for civilization. Major population developed over the river line systems due to rapid availability of sufficient and fresh amount of water but reliable and sustainable supply of fresh water in this era is a challenge due to rapid industrialization and human activities (Abdul et al. 2015; Carolin et al. 2017). The human population and their activities are increasing dramatically; consequently a large amount of fresh water would be required for the newly added people (Siddiqui and Chaudhry 2017a). In addition, contaminant released in water due to rapid industrialization, agricultural activities, geological activities and other human activities are deteriorating the water quality continuously. WHO, environmental agencies, government authorities, scientists, and academicians all over the world are worried and serious over the issue of water contamination. Thousands of organic, inorganic and biological species have been reported as water contaminants (Gao and Zhou 2000; Naushad 2014; Sang et al. 2003; Siddiqui et al. 2018). Heavy metals are among them which show serious adverse effects and toxicities; with lethal and carcinogenic effect, and cause the large damage to ecosystem and human health (Al-Othman et al. 2012; Carolin et al. 2017; Chaudhry et al. 2017a, b, c; Robinson 2017). Heavy metals having high specific gravity are found in earth crust and are non-biodegradable. They accumulate in food chain and soft and hard tissues of human body and get stored for long term, and affect the growth and development of the target organisms (Carolin et al. 2017; Robinson 2017; Siddiqui et al. 2017). The toxicities of various heavy metals are given in Table 1.

## 2 Arsenic Contamination and Toxicity

Arsenic contamination in water is becoming a severe problem for many countries particularly Asian countries such as Bangladesh, China, India, Pakistan, and Taiwan. The people of these countries are living in threat of arsenic (Bowell et al. 2014; Chaudhry et al. 2017b, c; Kao et al. 2013; Ng et al. 2003). Bangladesh and West Bengal province of India is the most affected zone of arsenic.

Arsenic inhalation through water is generally associated with skin lesions and hyperkeratosis like adverse effects (Matschullat 2000). Long-term exposure of arsenic contamination through water, affects the functioning of nervous and cardiovascular systems, and also causes cancers of many types (Abdul et al. 2015; Biswas et al. 2008; Siddiqui and Chaudhry 2017a, b, c, d; Watanabe et al. 2017). Moreover, arsenic alters the cell calcium signals; induce the oxidative stress, affect the cell mitochondrial function, and cell cycle progression (Abdul et al. 2015; Flora 2011; Kulshrestha et al. 2014).

Arsenic is found frequently in soil and rocks in the minerals form, which gets mobilized into ground water by natural weathering, geochemical reactions, biological activities, volcanic emissions and anthropogenic activities like mineralization, mining and smelting (Chaudhry et al. 2016a; Siddiqui and Chaudhry 2017a, b). Therefore, to control the arsenic effect, removal of arsenic from wastewater or drinking water is the best option to safe millions of people across the world. Various treatment techniques such as oxidation-coagulation, electro-coagulation and co-precipitation, oxidation-precipitation, reverse osmosis, electro dialysis, and ion exchange are being utilized. However, these techniques are inconvenient, require large space and are very costly (Anastopoulos et al. 2017; Chaudhry et al. 2016b; Devi and Saroha 2017; Mohan and Pittman 2007).

Adsorption being inexpensive; does not involve sophisticated instrumentation and do not require long procedure (Alqadami et al. 2016; Khan et al. 2015; Sharma et al. 2017). The process is simple, safe to handle and effectively work at low and high arsenic concentration in water (Gupta et al. 2009; Han et al. 2013; Mondal et al. 2007; Maliyekkal et al. 2009). Therefore, adsorption can be the better option to clean the arsenic contaminated water at different scales ranging from household module to community plants.

### 3 Adsorption Technology

Adsorption is a well-known water purification technology which involves the chemical or physical interaction between pollutant and solid surface, where solid surface is known as adsorbent and should have low particle size, high surface area, high active sites for higher removal capacity for pollutants (Bai et al. 2010; Fendorf et al. 1997; Johnston et al. 2016; Khan et al. 2013; Mohan and Pittman 2007; Sansone et al. 2013; Sherman and Randall 2003; Su et al. 2017). Large number of adsorbents have been utilized for removal of arsenic species (arsenite,  $\text{As}^{3+}$  and arsenate,  $\text{As}^{5+}$ ) but the arsenite,  $\text{As}^{3+}$  removal requires pre-oxidation of  $\text{As}^{3+}$  to  $\text{As}^{5+}$  using oxidizing agents, which makes the process costly and sometimes produce unhealthy by-products (Siddiqui and Chaudhry 2017a; Zhang et al. 2007). Therefore, to avoid the pre-oxidation step using costly oxidizing agents, various solid materials with oxidative properties have been developed (Siddiqui and Chaudhry 2017a, c).

Among the various materials graphene oxide provides high surface area and porosity, and strong active sites which can easily trap arsenic from water

(Peng et al. 2017; Platero et al. 2017; Kumar et al. 2014; Sheshmani et al. 2015). Graphene contains hydrophobic surface while large acidic groups are attached on the graphene oxide surface which results greater attraction for cations (Zhou et al. 2014). Abundant oxygenic groups such as epoxy, hydroxyl, and carboxyl are attached on the graphitic backbone of GO which protrude from its surface and can easily interact with the pollutants via coordination, electrostatic, and covalent interactions (Ray et al. 2017; Peng et al. 2017; Machida et al. 2006). Therefore, GO based adsorbents can be the best choice for researchers for arsenic removal. To ease the further study we have incorporated valuable literature here in this chapter. The objective of this chapter is to discuss the latest status of GO and its modified forms. Further, to inspire the environmental community, various GO based adsorbents, their adsorption capacity for arsenic, and comparative study has been incorporated. This chapter will help scientist community for the commercial application of the GO.

## 4 Graphene Oxide

Graphite oxide, also known as graphitic oxide or graphitic acid, is the compound of carbon, oxygen, and hydrogen. Graphite on oxidation with strong oxidizing agents like  $\text{KMnO}_4$  gives the Graphite oxide (GrO). GrO is normally yellow colour bulk solid having layer structure of graphite. GrO dispersed in alkaline solutions and produce the monolayer sheets which are known as graphene oxide (Wang et al. 2013; Bian et al. 2015; Gao et al. 2011).

Three approaches have been made for the preparation of GrO, such as Brodie, Staudenmaier and Hummers process. Brodie (1859) suggested that GrO can be prepared by oxidation of graphite powder with mixture of potassium per chlorate and concentrated nitric acid in water. Staudenmaier (1898) reported the preparation of GrO through the oxidation of graphite with mixture of sulfuric acid, nitric acid and potassium per chlorate. A similar approach was attempt by the Hummers and Offeman (1958) using solution of concentrated sulfuric acid, sodium nitrate and potassium permanganate. Obtained layer structure of GrO can easily be converted into the GO through mechanical stirring or ultrasonic process.

Actually, distance between the graphitic layers of GrO increases with increase in the oxygenen functional groups, and therefore, the interaction between the layers decreases which enhances the probability of formation of monolayer GO (Brodie 1859; Hummers and Offeman 1958; McAllister et al. 2007; Schniepp et al. 2006; Staudenmaier 1898).

#### 4.1 Preparation of GO and It's Composite

Recently, Hummers method have been modified which is frequently being used for the preparation of GO. In brief, certain amount of graphite flaks was dissolved into the solution of concentrated  $\text{H}_2\text{SO}_4:\text{H}_3\text{PO}_4$  (360:40 mL) under continuous stirring. Further,  $\text{KMnO}_4$  was added slowly to the suspension under vigorous stirring for 36 h at 50 °C, thus reddish suspension was obtained, cooled to room temperature, and added ~400 mL ice water containing 3.0 mL of 30%  $\text{H}_2\text{O}_2$  into the suspension under continues stirring until uniform mixture was obtained. Afterward, suspension was centrifuged, washed and dried (Kumar et al. 2014).

Due to the presence of oxygenous groups onto the surface, GO shows high adsorption capacity for water pollutants, but recovery of exhausted GO is not easy and require costly process such as centrifugation and filtration. This problem can be resolved by the modification of GO with magnetic particles. Large number magnetic GO have been utilized, that permit the use of bare GO in large-scale water treatment. Large numbers of magnetic GO have been developed by the simple co-precipitation method (Kumar et al. 2014).

Kumar et al. (2014) reported the preparation of magnetic  $\text{GO-MnFe}_2\text{O}_4$  nano-hybrid. In brief, 3.0 g GO was ultrasonically dispersed in 400 mL of water, then certain amount of ferric chloride ( $\text{FeCl}_3 \cdot 6\text{H}_2\text{O}$ ) and manganese sulfate ( $\text{MnSO}_4 \cdot \text{H}_2\text{O}$ ) were added to the GO solution and stirred for 0.5 h. Afterwards, the temperature of the reaction was increased up to 80 °C and pH of solution was adjusted to 10.5 by addition of 8 M NaOH solution, under continuous stirring. The reaction was continued for 5 min, and then cooled to room temperature and resulting precipitate was magnetically separated, washed and dried. Similarly, approaches were adopted for  $\text{FeO}_x\text{-GO}$  (Su et al. 2017) and  $\text{a-FeOOH@GCA}$  (Fu et al. 2017). One more attempt was made to improve the adsorption capacity of GO by the functionalization of GO. The functionalized GO surface have large number of oxygen atoms on the graphitic backbone, which provide the large number of active sites for charged ions (Fig. 1) (License No. 4147561017088) (Kumar and Jiang 2016).

In brief, 1.0 g of GO was dispersed in 50 mL thionyl chloride ( $\text{SOCl}_2$ )-dimethylformamide (DMF) solutions and then refluxed for 24 h at 60 °C. The obtained precipitate of  $\text{GO-COCl}$  was centrifuged, washed with tetrahydrofuran (THF) and

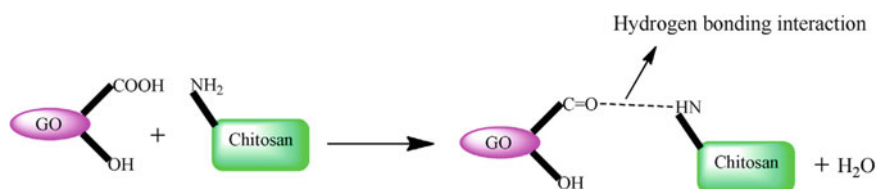


**Fig. 1** Hydrogen-bonding interaction between GO and chitosan. Reprinted with permission from Kumar and Jiang (2016) Copyright (2016) Elsevier (License No. 4147561017088)

dried under the vacuum. Afterwards, 1.0 g of GO-COCl was slowly added into the chitosan solutions (0.5 g of chitosan in 10 mL of 1% (v/v) acetic acid solutions) under the continues stirring for 10 min to get uniform mixture. The obtained mixture was slowly heated up to 50 °C and stirred for 3 h, and the resulting mixture was washed with acetone several times, filtered, and dried under vacuum (Kumar and Jiang 2016).

## 4.2 Characterization of GO

Preparation of GO and its composites was confirmed by FT-IR, Raman, and XRD techniques. Characteristic absorption peak of FT-IR spectrum of GO has shown in Table 2, which is clearly indicating the formation of GO and presence of oxygenated groups on a graphene matrix which grown for further modification.

Kumar et al. (2014) reported the characteristic absorption peaks at 1729, 1620, 1415, 1046, and 1236  $\text{cm}^{-1}$  for FTIR spectrum of GO (Fig. 2) (License No. 4147600394062). The C=O group is confirmed by the appearance of peak at 1729  $\text{cm}^{-1}$  in IR spectrum and C=C stretching was assigned by the appearance of peak at 1620  $\text{cm}^{-1}$ .

The absorption frequency at 1415  $\text{cm}^{-1}$  confirms C–H deformation bond. A band at 1046 and 1236  $\text{cm}^{-1}$  was appeared due to C–O stretching vibration for epoxy and alkoxy groups, respectively. Similar result was observed by (Khatamian et al. 2017; Kumar and Jiang 2016; Peng et al. 2017). Su et al. (2017) confirmed the distribution of iron oxide species onto GO matrix by assigning the absorption peaks for Fe–O, between the 750–400  $\text{cm}^{-1}$ . The formation of  $\text{FeO}_x$ -GO nano-composite was confirmed by the two bands at 552 and 442  $\text{cm}^{-1}$  for Fe–O and one band at 1578  $\text{cm}^{-1}$  for C=C stretch in GO. FTIR spectrum of GO-MnFe<sub>2</sub>O<sub>4</sub> (Fig. 2) exhibited absorption peaks at 490 and 577  $\text{cm}^{-1}$  due to M–O stretching vibrations of manganese ferrite (Kumar et al. 2014). Similar result was observed for (Huang et al. 2011; Kumar et al. 2014; Marcano et al. 2010) studies. The XRD spectrum of GO gives the characteristic peak at  $2\theta = 9.4\text{--}10.50^\circ$  corresponding to (001) plane of GO.

**Table 2** Characteristics absorption peaks for GO

Stretching frequency	Information (Khatamian et al. 2017; Kumar et al. 2014; Kumar and Jiang 2016; Peng et al. 2017)
3420–3200	V (O–H) stretching
2850–2950	Hydrogen bonding with oxygenous groups
1710–1730	V (C=O) stretching
1620–1640	V (C=C) in-plane stretching
1415–1550	V (O–H) deformation
1230–1400	V (C–O) Alkoxy stretching
1020–1070	V (C–O) Epoxy stretching

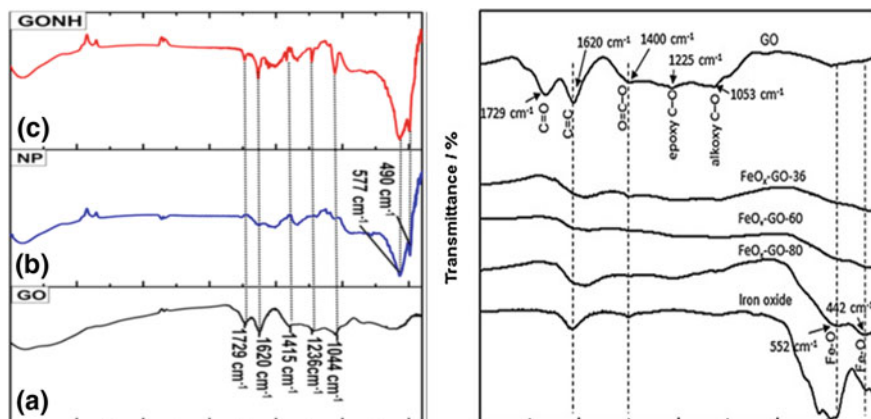


**Fig. 2** FTIR spectrum of GO and its composites. Reprinted with permission from **a** Kumar et al. (2014) Copyright (2014) American Chemical Society, **b** Su et al. (2017) Copyright (2017) Elsevier (License No. 4147600394062)

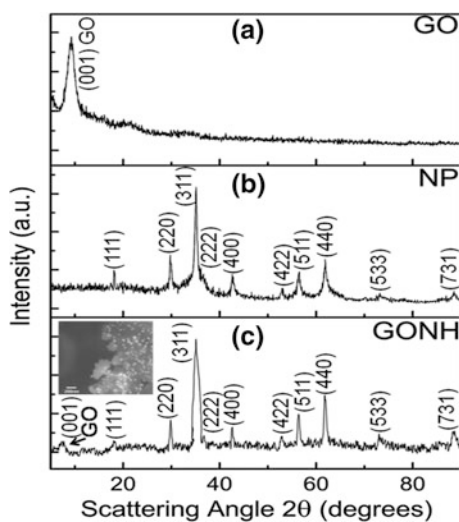


**Fig. 3** XRD spectra of GO,  $\text{MnFe}_2\text{O}_4$  and its composites ( $\text{GO-MnFe}_2\text{O}_4$ ). Reprinted with permission from **a** Kumar et al. (2014) Copyright (2014) American Chemical Society

After treatment of GO with metal, the diffraction intensity decreased which indicates the decline in crystalline structure. This was due to the bonding between the metal and GO. The similar result was also obtained for intramolecular or intermolecular hydrogen bonding interaction between the polymers and GO (Huang et al. 2011; Kumar et al. 2014; Kumar and Jiang 2016; Marcano et al. 2010). XRD pattern of GO and its composite is given in Fig. 3.

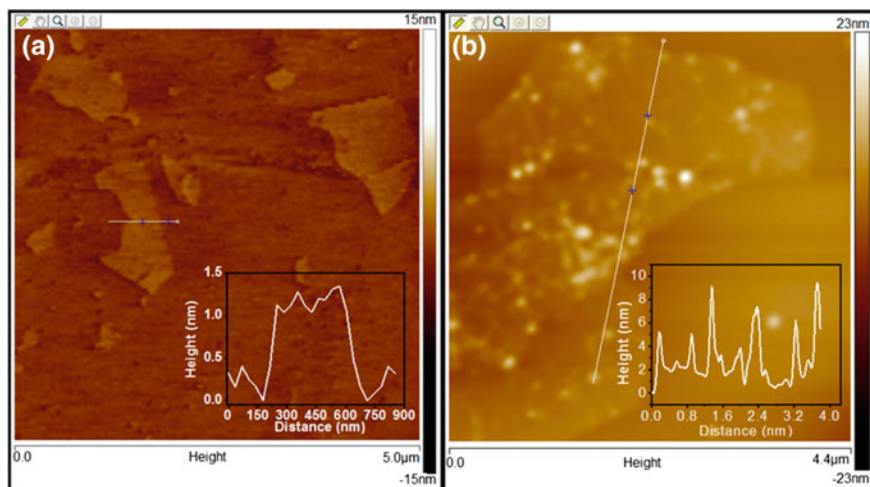


**Fig. 4** Atomic force microscopy (AFM) of **a** GO and **b** its composites (GO-MnFe<sub>2</sub>O<sub>4</sub>). Reprinted with permission from **a** Kumar et al. (2014) Copyright (2014) American Chemical Society

The average flake size and average thickness of GO flake was measured  $\sim 2 \mu\text{m}$  and  $\sim 1\text{--}2 \text{ nm}$ , respectively, using AFM (Fig. 4) (Huang et al. 2011; Kumar et al. 2014; Marcano et al. 2010).

Raman spectra has been widely used to characterize GO and GO based materials. Raman spectrum of GOs showed two prominent peaks at  $1580\text{--}1620$  and  $1340\text{--}1365 \text{ cm}^{-1}$  corresponding to the first order E<sub>2g</sub> mode from sp<sup>2</sup> carbon domains (G-band) and disorder mode (D-band), respectively. Kumar and Jiang (2016) of GO which showed strong peaks at  $1610$  and  $2445 \text{ cm}^{-1}$  related to G band and D' band, and one broad peak at  $1360 \text{ cm}^{-1}$  corresponding to D band.

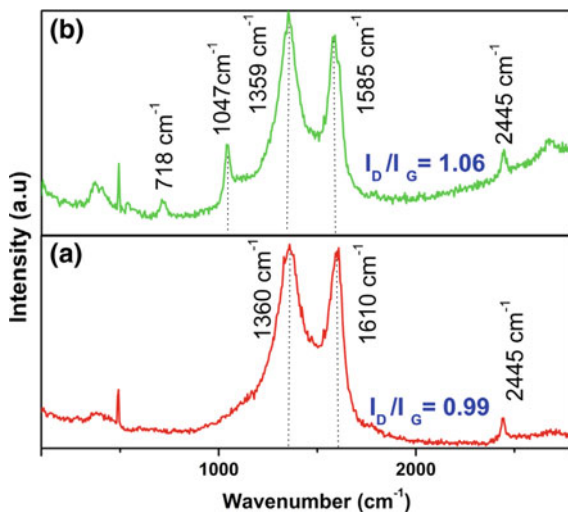
The functionalization of GO with chitosan shows two new peaks which emerged at  $718$  and  $1047 \text{ cm}^{-1}$  due to the interaction of COOH of the GO and OH group of chitosan (Fig. 5) (License No. 4147561017088). Similar results were reported by Chen et al. (2013), Kumar et al. (2014), Yang et al. (2013). The morphology of GO and their composites has been characterized from the SEM and TEM images by Chen et al. (2013), Kumar et al. (2014), Su et al. (2017), Yang et al. (2013).

## 5 GO as Adsorbent for Arsenic

Iron oxide loaded graphene oxide, magnetite (Fe<sub>3</sub>O<sub>4</sub>)-graphene oxide, magnetite (Fe<sub>3</sub>O<sub>4</sub>)-reduced graphene oxide, magnetite (Fe<sub>3</sub>O<sub>4</sub>)-reduced graphite oxide-MnO<sub>2</sub>, graphene-FeMnO<sub>x</sub>, and hydrous cerium oxide-graphene nano-composite are well known graphene based nano-composites that have been used for arsenic remediation (Kumar et al. 2014; Yu et al. 2015). These composites are magnetic in nature,



**Fig. 5** Raman spectrum of **a** GO and **b** its composites (GO-Chitosan). Reprinted with permission from Kumar and Jiang (2016) Copyright (2016) Elsevier (License No. 4147561017088)



show large sorption capacity towards arsenic and highly effective at various pHs, low concentration, and in the presence of competitive ions.

In comparison to virgin  $\text{MnFe}_2\text{O}_4$  nanoparticles, graphene oxide- $\text{MnFe}_2\text{O}_4$  nano-composite removed much higher As(III) and As(V). The maximum sorption capacity of graphene oxide- $\text{MnFe}_2\text{O}_4$  for As(III) and As(V) was recorded as 146 and 207 mg/g, respectively (Kumar et al. 2014). In addition, magnetite ( $\text{Fe}_3\text{O}_4$ )-reduced graphene oxide- $\text{MnO}_2$  nano-composite removed 14 mg/g of As(III) and 12 mg/g of As(V) (Xubiao et al. 2012), and graphene- $\text{FeMnO}_x$  removed 10.20 mg/g of As(III) and 11.50 mg/g of As(V) due to electrostatic interaction and pre-oxidation step (Jin et al. 2015). Yoon et al. (2016) reported the preparation of  $\text{Fe}_3\text{O}_4$ -graphene oxide composite (M-GO) and  $\text{Fe}_3\text{O}_4$ -reduced graphene oxide composite (M-rGO) (Fig. 6), investigated its arsenic removal capacity, and reached to the result that M-GO showed higher removal capacity for both As(III) and As(V) than M-rGO.

$\beta$ -FeOOH incorporated carboxylic graphene oxide nano-composite  $\beta$ -FeOOH@GO-COOH nanocomposite has removed 100% arsenic ions from water. The composite has shown tremendous adsorption efficiency even after 20 successive adsorption-desorption cycles, and removed >80% of both As(III) and As(V) from given initial concentration (Chen et al. 2015). The bonding between the  $\beta$ -FeOOH@GO-COOH and As(III), and As(V) has shown in Fig. 7.  $\beta$ -FeOOH@GO-COOH was also effective in the presence of 2000-fold of  $\text{SO}_4^{2-}$ ,  $\text{NO}_3^-$ ,  $\text{Cl}^-$  and  $\text{Mg}^{2+}$  ions, and provided 90% removal efficiency for 5 successive cycles. Maximum adsorption capacity for  $\beta$ -FeOOH@GO-COOH was found to be 77.5 and 45.7 mg/g for As(III) and As(V) ions, respectively (Chen et al. 2015).

Khatamian et al. (2017) reported the preparation of different composites of GO and RGO viz magnetite ( $\text{Fe}_3\text{O}_4$ )/RGO, magnetite ( $\text{Fe}_3\text{O}_4$ )/RGO/Cu-ZEA, GO/Cu-ZEA, and magnetite ( $\text{Fe}_3\text{O}_4$ )/GO/Cu-ZEA using solvothermal method with Cu-exchanged zeolite A (Cu-ZEA) and magnetite nanoparticles ( $\text{Fe}_3\text{O}_4$ ). This work was done for the

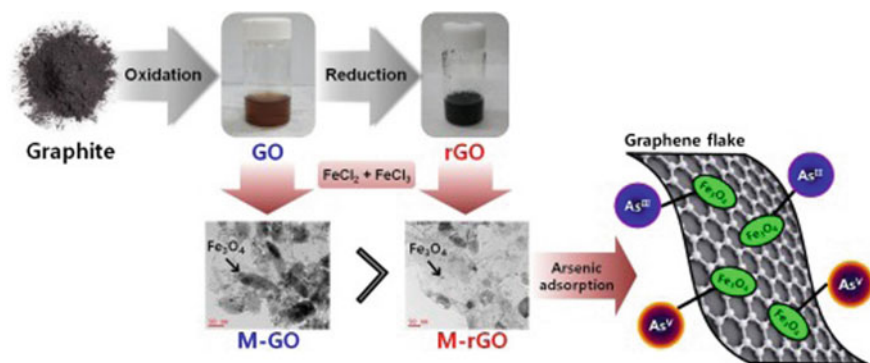


**Fig. 6** Preparative steps of magnetite-GO and magnetite-rGO nano-composite and their adsorption activity for As(III) and As(V). Reprinted with permission from Yoon et al. (2016) Copyright (2016) Elsevier (License No. 4147590561897)

improvement in the adsorption capacity of GO, RGO, magnetite ( $\text{Fe}_3\text{O}_4$ ) nanoparticles and Cu-ZEA. Among them magnetite ( $\text{Fe}_3\text{O}_4$ )/RGO/Cu-ZEA had the highest specific surface area thus they have shown the highest removal capacity for arsenic. The adsorption kinetics data followed the pseudo-second-order kinetic model. Similarly, Su et al. (2017) reported the synthesis  $\text{FeO}_x$ -GO nano-composites with different wt% (36–80 wt%) iron oxide content and further utilized for arsenic removal. GO sheets were prepared by an improved Hummers method and then iron oxide was incorporated on the GO through Co-precipitation reaction. With increased in the wt% of  $\text{FeO}_x$  on GO, the surface area for  $\text{FeO}_x$ -GO also increased, and iron oxide content of 80 wt% ( $\text{FeO}_x$ -GO-80) having predominant mesopore structures has highest surface area and consequently higher adsorption sites. Therefore,  $\text{FeO}_x$ -GO-80 showed maximum adsorption capacity of 147 and 113 mg/g for As(III) and As(V), respectively, which was highest among all the reported iron oxide-GO/reduced GO composite adsorbents.  $\text{FeO}_x$ -GO-80 removed  $\sim 100\%$  of arsenic from initial concentration of 118 and 108  $\mu\text{g/L}$ , of As(III) and As(V).

The mass production of non-oxidative graphene and magnetite/non-oxidative graphene (M-nOG) composite has been reported by Yoon et al. (2017) for arsenic removal. The M-nOG showed greater adsorption capacity for arsenic. The batch experiment was performed to evaluate the adsorption capacity of M-nOG for arsenic in terms of pH, temperature, competing anions, and humic acid. As(III) was largely influenced by the surface complexation while As(V) showed intraparticle diffusion mechanism. The repetitive reuse and regeneration of M-nOG were performed.

Further, three dimension (3D)-magnetite ( $\text{Fe}_3\text{O}_4$ )-graphene macroscopic composites have been utilized as adsorbents for the removal of arsenic from low level (Guo et al. 2015). 3D-graphene macroscopic composite was synthesized through the self-assembly of GO nanosheets with polydopamine and magnetite ( $\text{Fe}_3\text{O}_4$ ) nanoparticles under the basic conditions at low temperature. Polydopamine strengthen the 3 Dimension-graphene based macroscopic architect as well as enhanced the load and binding ability of magnetite ( $\text{Fe}_3\text{O}_4$ ) nanoparticles.

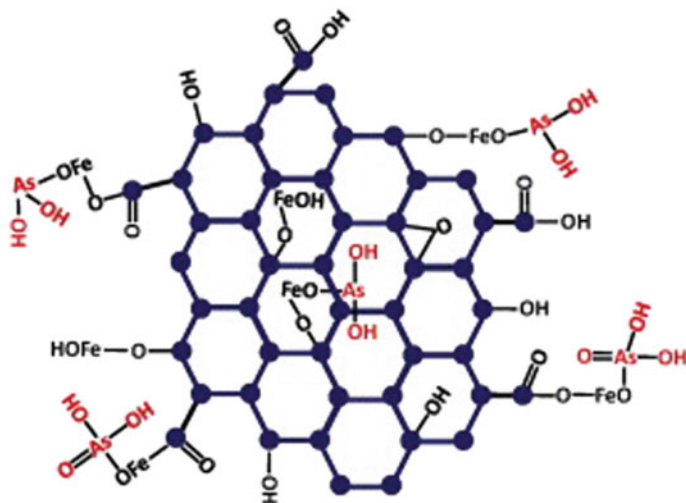


**Fig. 7** The bonding between  $\beta$ -FeOOH@GO-COOH and As(III), and As(V). Reprinted with permission from Chen et al. (2015) Copyright (2015) Elsevier (License No. 4147590927555)

Graphene based metal and metal oxide composites such as single metal Ag-RGO,  $\text{Cu}_2\text{O}$ -RGO, and magnetite ( $\text{Fe}_3\text{O}_4$ )-RGO and bimetallic Ag- $\text{Cu}_2\text{O}$ -RGO, Ag-magnetite ( $\text{Fe}_3\text{O}_4$ )-RGO, and  $\text{Cu}_2\text{O}$ -magnetite ( $\text{Fe}_3\text{O}_4$ )-RGO have been utilized for the adsorptive removal of As(V) (Dubey et al. 2015). These adsorbents were synthesized hydrothermally using sodium borohydride as a reducing agent and sodium sorbate as a stabilizer. Similarly, Al and Fe-doped graphene was used for the removal of methylated As(III) and As(V) and their adsorption capacity was studied by quantum chemistry computations (Arriagada and Labbe 2016).

Kumar and Jiang (2016) reported the preparation of chitosan functionalized GOs which act as interactive sites due to the presence of one amino group and two hydroxyl groups on each glucosamine monomer of chitosan. The formation of chitosan functionalized GO was due to the electrostatic affinity between the amino group ( $\text{NH}_2$ ), primary and secondary hydroxyl groups ( $\text{CH}_2\text{OH}$ ,  $\text{CHOH}$ ) of the chitosan and surface of carboxyl ( $\text{COOH}$ ) and hydroxyl groups ( $\text{OH}$ ) on the GO. The chitosan functionalized GO worked as good host for incoming arsenic oxy-anion. Various interaction mechanism such as cation- $\pi$  interaction ( $\text{RNH}_3^+$ —aromatic  $\pi$  moiety), electrostatic interaction ( $\text{H}_2\text{AsO}_4^-$ ,  $\text{HAsO}_4^{2-}$ — $^+\text{NH}_3\text{R}$ ), and inter and intermolecular hydrogen bonding as well as anion- $\pi$  interaction ( $\text{R-COO}^-$ —aromatic  $\pi$  moiety), ( $\text{R-O}^-$ —aromatic  $\pi$  moiety) defined the interaction between arsenic and GO moieties. Mishra and Ramaprabhu (2011) prepared the graphene sheets by hydrogen induced exfoliation of graphitic oxide followed by functionalization and used for the removal of high concentration of inorganic species of arsenic As(III) and As(V) from aqueous solution using super capacitor based water filter. The maximum monolayer adsorption capacities for As(III) and As(V) were 142, and 139 mg/g, respectively, which were higher than other,

reported adsorbents. Graphene based super capacitor provides a solution for commercially feasible water filter.

Similarly,  $\beta$ -Cyclodextrins (CDs) functionalized GO ( $\beta$ -CDs@GO hybrid), magnetite ( $\text{Fe}_3\text{O}_4$ ) nanoparticles decorated with  $\beta$ -CDs-functionalized GO ( $\text{Fe}_3\text{O}_4$ - $\beta$ -CDs@GO hybrid),  $\beta$ -CDs-GO@ magnetite ( $\text{Fe}_3\text{O}_4$ ) nanoparticles and polyelectrolyte of poly (diallyldimethylammonium chloride) (pDADMAC) with paramagnetic anions based on  $\text{FeCl}_4$ -GO (Fe-polyDADMAC@GO) have been synthesized for the removal of arsenic from water. Kumar and Jiang (2017) reported the magnetically separable and recyclable magnetic nanoparticles decorated with  $\beta$ -cyclodextrin functionalized graphene oxide for As(III) and As(V) cleanup from water. Due to hydroxyl and carboxyl groups present on the surface of  $\beta$ -CDs-GO@ magnetite ( $\text{Fe}_3\text{O}_4$ ) nanoparticles and their superior magnetic property, this adsorbent showed excellent adsorption capacity for As(III) and As(V). Batch adsorption experiments were performed to demonstrate the maximum adsorption capacity of prepared adsorbent in terms of various parameters such as pH, temperature, and contact time. Adsorption isotherms and kinetics data were well described by Freundlich isotherm and the pseudo-second order kinetic models, respectively. Thermodynamics studies suggested that the reaction was feasible, spontaneous and endothermic. Adsorbent was regenerated using sodium hydroxide (NaOH) and was reutilized for two adsorption/desorption cycles.

Graphene-doped titanium nano tube coated to super paramagnetic nanoparticles (GN-MNP-TNT) was used to remove As(III) from their solutions (Lin et al. 2017). GO layers served as precursor and stabilizer for GN-MNP-TNT due to their excellent electron transfer capacities. TNT-doped graphene (GN-TNT) was prepared by hydrothermal method. GN-MNP-TNT could be tested for 4 consecutive adsorption/desorption cycle without major loss. After 4 cycle of regeneration adsorbent efficiency remained 83% which was much higher than other reported value in literature.

## 5.1 GO Coated Carbon Nanotubes

In addition to this, carbons nanotubes have also been incorporated with GO but limited number of literature is available. Goethite impregnated graphene oxide (GO)-carbon nanotubes (CNTs) aerogel ( $\alpha$ -FeOOH@GCA) was prepared for adsorptive removal of arsenic from water (Fu et al. 2017).  $\alpha$ -FeOOH@GCA was prepared by a facile self-assembly of GO-CNTs by in situ  $\text{Fe}^{2+}$  reduction method. Batch experiment was performed to investigate the adsorption capacity of prepared  $\alpha$ -FeOOH@GCA for different arsenic species like As(V), DMA, and *p*-ASA. The maximum adsorption capacities for As(V), DMA and *p*-ASA was obtained as 56.43, 24.43 and 102.11 mg/g which was much higher than (25.71, 8.03 and 14.52 mg/g) pristine  $\alpha$ -FeOOH, respectively. This was due to the incorporation of GO-CNTs, which not only hindered the aggregation of GO-CNTs but also inhibited the growth of  $\alpha$ -FeOOH nanoparticles and facilitated the diffusion and adsorption.

$\alpha$ -FeOOH@GCA showed excellent reusability with adsorption capacity, however, adsorption rate was affected by the presence of phosphate and silicate anions due to the similar anionic structure. The complex prepared between the arsenic species and the surface of  $\alpha$ -FeOOH@GCA was inner sphere complex.

Park et al. (2016) developed a feasible water flow filter with facilely functionalized magnetite ( $\text{Fe}_3\text{O}_4$ )-non-oxidative graphene/CNT composites for arsenic removal in household use for continuous purification of water. Feasible water flow filter filled with magnetite ( $\text{Fe}_3\text{O}_4$ )-functionalized non-oxidative graphene/CNT was fabricated through facile functionalization in a Couette-Taylor flow reactor. Couette-Taylor flow method allows the fast production of filters. magnetite ( $\text{Fe}_3\text{O}_4$ )-functionalized non-oxidative graphene/CNT composites as flow filter showed higher arsenic removal efficiency than when it was used in the batch experiment. This is due to its 3D-structure which enhanced the water flow pathway and the contact area with magnetite ( $\text{Fe}_3\text{O}_4$ ). Similarly, Roy et al. (2016) reported a Europium doped magnetic graphene oxide-MWCNT nanohybrid adsorbent for effective and rapid removal of As(III) and As(V) from real water samples. This adsorbent could be prepared by a combination of Eu-doped magnetic graphene oxide and gold nanoparticle functionalized multiwalled carbon nanotubes. Prepared nano-hybrid adsorbent having magnetic property (15,000 emu/g) showed extraordinary adsorption capacity as 320.0 and 298.0 mg/g for As(III) and As(V), respectively, and also showed excellent photo catalytic activity for oxidation of As(III) to As(V). Therefore, this adsorbent could be utilized for the conversion of highly toxic As(III) to less toxic As(V) as well as adsorptive removal of As(V). These were recently utilized GO based adsorbents, which could be effective for arsenic removal, however, more study is needed to make the process more convenient.

## 6 Conclusion and Future Prospects

The excellent adsorption performance, along with their low cost and convenient synthesis, makes GO and its composites highly promising for commercial applications in drinking water purification and wastewater treatment. Reusability, ease of magnetic separation, high removal efficiency, and fast kinetics make them very attractive and smart materials for the effective removal of heavy metals particularly arsenic from contaminated water. The experimental conditions and results for GO for arsenic remediation provide a way for further research and development of GO based adsorbent for others charged pollutants.

**Acknowledgements** The financial support from the University Grant Commission, UGC, India and Department of Chemistry, Jamia Millia Islamia, New Delhi, India, is gratefully acknowledged.

## References

- Abdul KS, Jayasinghe SS, Chandana EP, Jayasumana C, De-Silva PM (2015) Arsenic and human health effects: a review. *Environ Toxicol Pharmacol* 40:828–846
- AL-Othman ZA, Ali R, Naushad M, (2012) Hexavalent chromium removal from aqueous medium by activated carbon prepared from peanut shell: Adsorption kinetics, equilibrium and thermodynamic studies. *Chem Eng J* 184:238–247
- Alqadami AA, Naushad M, Abdalla MA et al (2016) Synthesis and characterization of Fe<sub>3</sub>O<sub>4</sub>@TSC nanocomposite: highly efficient removal of toxic metal ions from aqueous medium. *RSC Adv* 6:22679–22689
- Anastopoulos I, Karamesouti M, Mitropoulos AC, Kyzas GZ (2017) A review for coffee adsorbents. *J Mol Liq* 229:555–565
- Arriagada DC, Labbe AT (2016) Aluminum and iron doped graphene for adsorption of methylated arsenic pollutants. *Appl Surf Sci* 386:84–95
- Bai L, Ma XJ, Liu JF, Sun XM, Zhao DY, Evans DG (2010) Rapid separation and purification of nanoparticles in organic density gradients. *J Am Chem Soc* 132:2333–2337
- Bian Y, Bian ZY, Zhang JX, Ding AZ, Liu SL, Wang H (2015) Effect of the oxygen-containing functional group of graphene oxide on the aqueous cadmium ions removal. *Appl Surf Sci* 329:269–275
- Biswas BK, Inoue JI, Inoue K, Ghimire KN, Harada H, Ohto K, Kawakita H (2008) Adsorptive removal of As(V) and As(III) from water by a Zr(IV)-loaded orange waste gel. *J Hazard Mater* 154:1066–1074
- Bowell RJ, Alpers CN, Jamieson HE, Nordstrom DK, Majzlan J (2014) The environmental geochemistry of arsenic—an overview. *Rev Mineral Geochem* 79:1–16
- Brodie BC (1859) On atomic weight of graphite. *Philos Trans R Soc Lond* 149:249–259
- Carolin F, Kumar PS, Saravanan A, Joshiba GJ, Naushad M (2017) Efficient techniques for the removal of toxic heavy metals from aquatic environment: a review. *J Environ Chem Eng* 5:2782–2799
- Chaudhry SA, Khan TA, Ali I (2017a) Equilibrium, kinetic and thermodynamic studies of Cr(VI) adsorption from aqueous solution onto manganese oxide coated sand grain (MOCSG). *J Mol Liq* 236:320–330
- Chaudhry SA, Khan TA, Ali I (2017b) Zirconium oxide-coated sand based batch and column adsorptive removal of arsenic from water: Isotherm, kinetic and thermodynamic studies. *Egypt J Petrol* 26:553–563
- Chaudhry SA, Ahmed M, Siddiqui SI, Ahmed S (2016a) Fe(III)-Sn(IV) mixed binary oxide-coated sand preparation and its use for the removal of As(III) and As(V) from water: application of isotherm, kinetic and thermodynamics. *J Mol Liq* 224:431–441
- Chaudhry SA, Khan TA, Ali I (2016b) Adsorptive removal of Pb(II) and Zn(II) from water onto manganese oxide-coated sand: Isotherm, thermodynamic and kinetic studies. *Egypt J Basic App Sci* 3:287–300
- Chaudhry SA, Zaidi Z, Siddiqui SI (2017c) Isotherm, kinetic and thermodynamics of arsenic adsorption onto Iron-Zirconium Binary Oxide-Coated Sand (IZBOCS): modelling and process optimization. *J Mol Liq* 229:230–240
- Chaudhry SA, Siddiqui SI (2017) Arsenic removal from water using nano-composites: a review. *Cur Environ Eng*. <https://doi.org/10.2174/2212717804666161214143715>
- Chen J, Yao B, Li C, Shi G (2013) An improved Hummers method for eco-friendly synthesis of graphene oxide. *Carbon* 64:225–229
- Chen ML, Sun Y, Huo CB, Liu C, Wang JH (2015) Akaganeite decorated graphene oxide composite for arsenic adsorption/removal and its pre-concentration at ultra-trace level. *Chemosphere* 130:52–58
- Devi P, Saroha AK (2017) Utilization of sludge based adsorbents for the removal of various pollutants: a review. *Sci Total Environ* 578:16–33

- Dikilitas M, Karakas S, Ahmad P (2016) Chapter 3: effect of lead on plant and human DNA damages and its impact on the environment. *Plant Metal Interact* 41–67
- Dubey SP, Nguyen TTM, Kwon YN, Lee C (2015) Synthesis and characterization of metal-doped reduced graphene oxide composites, and their application in removal of *Escherichia coli*, arsenic and 4-nitrophenol. *J Indus Eng Chem* 29:282–288
- Fendorf SE, Grossl MJP, Sparks DL (1997) Arsenate and chromate retention mechanisms on goethite surface structure. *Environ Technol* 31:315–320
- Flora SJS (2011) Arsenic-induced oxidative stress and its reversibility. *Free Rad Bio Med* 51:257–281
- Fristachi A, Chaudhry H (2017) Cadmium. In: *International encyclopedia of public health* (vol 5, 2nd edn), pp 316–319
- Fu D, He Z, Su S, Xu B, Liu Y, Zhao Y (2017) Fabrication of  $\alpha$ -FeOOH decorated graphene oxide-carbon nanotubes aerogel and its application in adsorption of arsenic species. *J Colloid Interface Sci* 505:105–114
- Gao TY, Zhou ZY (2000) The simple denitrification and phosphate removal transformation for municipal waste water treatment plant. *J Tongji Uni (Sci)* 28:324–327
- Gao W, Majumder M, Alemany LB, Narayanan TN, Ibarra MA, Pradhan BK, Ajayan PM (2011) Engineered graphite oxide materials for application in water purification. *ACS Appl Mater Interfaces* 3:1821–1826
- Guo L, Ye P, Wang J, Fu F, Wu Z (2015) Three-dimensional Fe<sub>3</sub>O<sub>4</sub>-graphene macroscopic composites for arsenic and arsenate removal. *J Hazard Mater* 298:28–35
- Gupta A, Chauhan VS, Sankaramakrishnan N (2009) Preparation and evaluation of iron-chitosan composites for removal of As(III) and As(V) from arsenic contaminated real life groundwater. *Water Res* 43:3862–3870
- Ha E, Basu N, O'Reilly SB, Dórea JG, Chan HM (2017) Current progress on understanding the impact of mercury on human health. *Environ Res* 152:419–433
- Han C, Li H, Pu H, Yu H, Deng L, Huang S, Luo Y (2013) Synthesis and characterization of mesoporous alumina and their performances for removing arsenic (V). *Chem Eng J* 217:1–9
- Huang NM, Lim HN, Chia CH, Yarmo MA, Muhamad MR (2011) Simple room-temperature preparation of high-yield large-area graphene oxide. *Int J Nanomed* 6:3443–3448
- Hummers WS Jr, Offeman RE (1958) Preparation of graphitic oxide. *J Am Chem Soc* 80:1339
- Jin Z, Zimo L, Yu L, Ruiqi F, Shams AB, Xinhua X (2015) Adsorption behavior and removal mechanism of arsenic on graphene modified by iron-manganese binary oxide (FeMnO<sub>x</sub>/RGO) from aqueous solutions. *RSC Adv* 5:67951–67961
- Johnston SG, Burton ED, Moon EM (2016) Arsenic mobilization is enhanced by thermal transformation of schwertmannite. *Environ Sci Technol* 50:8010–8019
- Kao AC, Chu YJ, Hsu FL, Liao VHC (2013) Removal of arsenic from groundwater by using a native isolated arsenite-oxidizing bacterium. *J Contam Hydrol* 155:1–8
- Khan TA, Chaudhry SA, Ali I (2013) Thermodynamic and kinetic studies of As(V) removal from water by zirconium oxide coated marine sand. *Environ Sci Pollut Res* 20:5425–5440
- Khan TA, Chaudhry SA, Ali I (2015) Equilibrium uptake, isotherm and kinetic studies of Cd(II) adsorption onto iron oxide activated red mud from aqueous solution. *J Mol Liq* 202:165–175
- Khatamian M, Khodakarampoor N, Oskoui MS (2017) Efficient removal of arsenic using graphene-zeolite based composites. *J Colloid Interface Sci* 498:433–441
- Kulshrestha A, Jarouliya U, Prasad GBKS, Flora SJS, Bisen PS (2014) Arsenic-induced abnormalities in glucose metabolism: biochemical basis and potential therapeutic and nutritional interventions. *World J Trans Med* 3:96–111
- Kumar S, Nair RR, Pillai PB, Gupta SN, Iyengar MAR, Sood AK (2014) Graphene oxide-MnFe<sub>2</sub>O<sub>4</sub> magnetic nano-hybrids for efficient removal of lead and arsenic from water. *ACS Appl Mater Interfaces* 6:17426–17436
- Kumar SK, Jiang SJ (2016) Chitosan-functionalized graphene oxide: a novel adsorbent an efficient adsorption of arsenic from aqueous solution. *J Environ Chem Eng* 4:1698–1713
- Kumar SK, Jiang SJ (2017) Synthesis of magnetically separable and recyclable magnetic nanoparticles decorated with  $\beta$ -cyclodextrin functionalized graphene oxide an excellent adsorption of As(V)/(III). *J Mol Liq* 237:387–401

- Li P, Du B, Chan HM, Feng X (2015) Human inorganic mercury exposure, renal effects and possible pathways in Wanshan mercury mining area China. *Environ Res* 140:198–204
- Lin YJ, Cao WZ, Ouyang T, Chen BY, Chang CT (2017) Developing sustainable graphene-doped titanium nano tube coated to super paramagnetic nanoparticles for arsenic recovery. *J Taiwan Inst Chem Eng* 70:311–318
- Machida M, Mochimaru T, Tatsumoto H (2006) Lead(II) adsorption onto the graphene layer of carbonaceous materials in aqueous solution. *Carbon* 44:2681–2688
- Maliyekkal SM, Philip L, Pradeep T (2009) As(III) removal from drinking water using manganese oxide-coated-alumina: performance evaluation and mechanistic details of surface binding. *Chem Eng J* 153:101–107
- Marcano DC, Kosynkin DV, Berlin JM, Sinitskii A, Sun Z, Slesarev A, Alemany LB, Lu W, Tour JM (2010) Improved synthesis of graphene oxide. *ACS Nano* 4:4806–4814
- Matschullat J (2000) Arsenic in the geosphere—a review. *Sci Total Environ* 249:297–312
- McAllister MJ, Li JL, Adamson DH, Schniepp HC, Abdala AA, Liu J, Alonso MH, Milius DL, Car R, Prud'homme V (2007) *Chem Mater* 19:4396
- Mishra AK, Ramaprabhu S (2011) Functionalized graphene sheets for arsenic removal and desalination of sea water. *Desalination* 282:39–45
- Mohan D, Pittman CU Jr (2007) Arsenic removal from water/wastewater using adsorbents—a critical review. *J Hazard Mater* 142:1–53
- Mondal P, Balomajumder C, Mohanty B (2007) A laboratory study for the treatment of arsenic, iron, and manganese bearing ground water using Fe<sup>3+</sup> impregnated activated carbon: effects of shaking time, pH and temperature. *J Hazard Mater* 144:420–426
- Naushad M (2014) Surfactant assisted nano-composite cation exchanger: Development, characterization and applications for the removal of toxic Pb<sup>2+</sup> from aqueous medium. *Chem Eng J* 235:100–108
- Ng JC, Wang J, Shraim A (2003) Global health problems caused by arsenic from natural sources. *Chemosphere* 52:1353–1359
- Park WK, Yoon Y, Kim S, Yoo S, Do Y, Kang JW, Yoon DH, Yang WS (2016) Feasible water flow filter with facilely functionalized Fe<sub>3</sub>O<sub>4</sub>-non-oxidative graphene/CNT composites for arsenic removal. *J Environ Chem Eng* 4:3246–3252
- Peng W, Li H, Liu Y, Song S (2017) A review on heavy metal ions adsorption from water by graphene oxide and its composites. *J Mol Liq* 230:496–504
- Platero E, Fernandez ME, Bonelli PR, Cukierman AL (2017) Graphene oxide/alginate beads as adsorbents: influence of the load and the drying method on their physicochemical-mechanical properties and adsorptive performance. *J Colloid Interface Sci* 491:1–12
- Rasheed H, Kay P, Slack R, Gong YY, Carter A (2017) Human exposure assessment of different arsenic species in household water sources in a high risk arsenic area. *Sci Total Environ* 584–585:631–641
- Ray SK, Majumdera C, Saha P (2017) Functionalized reduced graphene oxide (RGO) for removal of fulvic acid contaminant. *RSC Adv* 7:21768–21779
- Robinson T (2017) Removal of toxic metals during biological treatment of landfill leachates. *Waste Manage* 63:299–309
- Rodríguez J, Mandalunis PM (2016) Effect of cadmium on bone tissue in growing animals. *Exp Toxicol Pathol* 68:391–397
- Roy E, Patra S, Madhuri R, Sharma PK (2016) Europium doped magnetic graphene oxide-MWCNT nanohybrid for estimation and removal of arsenate and arsenite from real water samples. *Chem Eng J* 299:244–254
- Sang JQ, Zhang XH, Wang ZS (2003) Improvement of organics removal by bio-ceramic filtration of raw water with addition of phosphorus. *Water Res* 37:4711–4718
- Sansone V, Pagani D, Melato M (2013) Chronic arsenicals dermatoses from tube-well water in West Bengal during 1983–87. *Clin Cases Miner Bone Metab* 10:34–40
- Schniepp HC, Li JL, McAllister MJ, Sai H, Alonso MH, Adamson DH, Prud'homme RK, Car R, Saville DA, Aksay IA (2006) Functionalized graphene sheets derived from splitting graphite oxide. *J Phys Chem B* 110:8535–8539



- Sharma G, Naushad M, Al-Muhtaseb AH, Kumar A, Khan MR, Kalia SS, Bala M, Sharma A (2017) Fabrication and characterization of chitosan-crosslinked-poly(alginate) nanohydrogel for adsorptive removal of Cr(VI) metal ion from aqueous medium. *Int J Biol Macromol* 95:484–493
- Sherman DM, Randall SR (2003) Surface complexation of arsenic (V) to iron(III) (hydr)oxides: structural mechanism from ab initio molecular geometries and EXAFS spectroscopy. *Geochim Cosmochim Acta* 67:575–580
- Sheshmani S, Nematzadeh MA, Shokrollahzadeh S, Ashori A (2015) Preparation of graphene oxide/chitosan/FeOOH nanocomposite for the removal of Pb (II) from aqueous solution. *Int J Biol Macromol* 80:475–480
- Siddiqui SI, Chaudhry SA, Islam SU (2017) Green adsorbents from plant sources for the removal of arsenic: an emerging wastewater treatment technology. In *plant-based natural products: derivatives and applications*, Ed. Islam SU, John Wiley & Sons, Inc, pp. 193–215
- Siddiqui SI, Chaudhry SA (2017a) Arsenic removal from water using nano-composites: a review. *Cur Environ Eng* 4:81–102
- Siddiqui SI, Chaudhry SA (2017b) Arsenic: toxic effects and remediation. In *advanced materials for wastewater treatment*, Ed. Islam SU, John Wiley & Sons, Inc, pp. 1–27
- Siddiqui SI, Chaudhry SA (2017c) Iron oxide and its modified forms as an adsorbent for arsenic removal: a comprehensive recent advancement. *Process Saf Environ Prot* 111:592–626
- Siddiqui SI, Chaudhry SA (2017d) Removal of arsenic from water through adsorption onto metal oxide-coated material. *Mater Res Found* 15:227–276
- Siddiqui SI, Ravi R, Rathi G, Tara N, Islam SU, Chaudhry SA (2018) Decolorization of textile wastewater using composite materials. In *nano materials in the wet processing of textiles*, Ed. Islam SU, Butola BS, John Wiley & Sons, Inc, pp. 187–218
- Staudenmaier L (1898) Verfahren zur darstellung der graphitsaure. *Ber Dtsch Chem Ges* 31:1481–1487
- Su H, Ye Z, Hmidi N (2017) High-performance iron oxide–graphene oxide nanocomposite adsorbents for arsenic removal efficient removal of arsenic using graphene-zeolite based composites. *Colloids Surf A: Physicochem Eng Asp* 522:161–172
- Wang H, Yuan X, Wu Y, Huang H, Zeng G, Liu Y, Wang X, Lin N, Qi Y (2013) Adsorption characteristics and behaviors of graphene oxide for Zn (II) removal from aqueous solution. *Appl Surf Sci* 279:432–440
- Watanabe CH, Monteiro ASC, Gontijo ESJ, Lira VS, Bueno CDC, Kumar NT, Fracácio R Rosa AH (2017) Toxicity assessment of arsenic and cobalt in the presence of aquatic humic substances of different molecular sizes. *Ecotoxicol Environ Saf* 139:1–8
- Xubiao L, Cheng W, Shenglian L, Ruizhi D, Xinman T, Guisheng Z (2012) Adsorption of As(III) and As(V) from water using magnetite Fe<sub>3</sub>O<sub>4</sub>-reduced graphite oxide-MnO<sub>2</sub> nano composites. *Chem Eng J* 187:45–52
- Yang G, Cao J, Li L, Rana RK, Zhu JJ (2013) Carboxymethyl chitosan-functionalized graphene for label free electrochemical cytosensing. *Carbon* 51:124–133
- Yoon Y, Park WK, Hwang TM, Yoon DH, Yang WS, Kang JW (2016) Comparative evaluation of magnetite–graphene oxide and magnetite-reduced graphene oxide composite for As(III) and As (V) removal. *J Hazard Mater* 304:196–204
- Yoon Y, Zheng M, Ahn YT, Park WK, Yang WS, Kang JW (2017) Synthesis of magnetite/non-oxidative graphene composites and their application for arsenic removal. *Sep Pure Technol* 178:40–48
- Yu L, Ma Y, Ong CN, Xie J, Liu Y (2015) Rapid adsorption removal of arsenate by hydrous cerium oxide–graphene composite. *RSC Adv* 5:64983–64990
- Zhang G, Qu J, Liu H, Liu R, Wu R (2007) Preparation and evaluation of a novel Fe-Mn binary oxide adsorbent for effective arsenite removal. *Water Res* 41:1921–1928
- Zhou Q, Zhong YH, Chen X, Liu JH, Huang XJ, Wu YC (2014) Adsorption and photo catalysis removal of fulvic acid by TiO<sub>2</sub>-graphene composites. *J Mater Sci* 49:1066–1075